nature medicine

Effective gene therapy with nonintegrating lentiviral vectors

Rafael J Yáñez-Muñoz[1,2,10,11], Kamaljit S Balaggan[3,11], Angus MacNeil[3], Steven J Howe[1], Manfred Schmidt[4,5], Alexander J Smith[3], Prateek Buch[3], Robert E MacLaren[3], Patrick N Anderson[6], Susie E Barker[3], Yanai Duran[3], Cynthia Bartholomae[4,5], Christof von Kalle[4,5,7], John R Heckenlively[8], Christine Kinnon[1], Robin R Ali[1,3] & Adrian J Thrasher[1,9]

Retroviral and lentiviral vector integration into host-cell chromosomes carries with it a finite chance of causing insertional mutagenesis[1]. This risk has been highlighted by the induction of malignancy in mouse models, and development of lymphoproliferative disease in three individuals with severe combined immunodeficiency–X1 (refs. 2,3). Therefore, a key challenge for clinical therapies based on retroviral vectors is to achieve stable transgene expression while minimizing insertional mutagenesis. Recent *in vitro* studies have shown that integration-deficient lentiviral vectors can mediate stable transduction[4–6]. With similar vectors, we now show efficient and sustained transgene expression *in vivo* in rodent ocular and brain tissues. We also show substantial rescue of clinically relevant rodent models of retinal degeneration. Therefore, the high efficiency of gene transfer and expression mediated by lentiviruses can be harnessed *in vivo* without a requirement for vector integration. For therapeutic application to postmitotic tissues, this system substantially reduces the risk of insertional mutagenesis.

Retroviruses and retroviral vectors can be rendered integration defective by mutations in the integrase coding sequence. Class II mutations in the gene encoding integrase have pleiotropic effects, but class I mutations result in normal DNA synthesis, integration failure and accumulation of DNA in the cell nucleus as double-stranded circles[7]. Two circular forms are produced from the unintegrated linear double-stranded DNA, presumed to be the result of intramolecular homologous recombination between long terminal repeats (LTRs; 1-LTR circle) or intramolecular end-joining (2-LTR circle)[8,9]. These circles lack replication signals and in cultured cells dilute as a consequence of cell division[10,11].

Class I integration-deficient lentiviral vectors have been reported to be inefficient for transduction of dividing cells *in vitro*[12,13]. More recently, prolonged gene expression has been shown in cultured nondividing primary rat neurons and growth-arrested fibroblasts, and in SV40 T antigen–expressing proliferating cells through the incorporation of episomal replication signals[4–6]. In contrast, direct administration of nonintegrating vectors based on human immunodeficiency virus (HIV) or feline immunodeficiency virus (FIV) has not previously resulted in significant expression *in vivo*[14–16]. In view of justified concerns relating to insertional mutagenesis, we chose to reevaluate *in vivo* transduction by integration-deficient lentiviral vectors in well-established rodent models of ocular gene therapy, a system permissive for expression from HIV-1–based and other lentiviral vectors.

The class I integration-deficient vectors used in this study carry a mutant D64V integrase which decreases integration of pseudotyped HIV-1 to 1/10,000 of wild type[17]. We produced paired integration-proficient and integration-deficient HIV-1 vectors using self-inactivating systems[18] (**Fig. 1a**,**b**). *In vitro* analyses showed that paired vectors had similar titers (**Supplementary Note** and **Supplementary Table 1** online). Integration-deficient *eGFP*-encoding vectors led to transient green fluorescence in a permissive cell line (**Supplementary Note** and **Supplementary Fig. 1** online). As expected, Southern blot assays showed the disappearance of integration-deficient vector over time (**Supplementary Note** and **Supplementary Fig. 1** online).

We investigated the ocular transduction patterns of paired integration-proficient and integration-deficient vectors in mice using *eGFP*-encoding vectors with various promoters and regulatory elements (**Fig. 1a,c**). We observed identical spatial and temporal transduction patterns regardless of integration proficiency or vector configuration. These patterns were consistent with previous studies

[1]Molecular Immunology Unit, Institute of Child Health, University College London, 30 Guilford Street, London WC1N 1EH, UK. [2]Centre for Medical Oncology, Institute of Cancer and the CR-UK Clinical Centre, Barts and The London, Queen Mary's School of Medicine and Dentistry, John Vane Science Centre, Charterhouse Square, London EC1M 6BQ, UK. [3]Division of Molecular Therapy, Institute of Ophthalmology, University College London, 11-43 Bath Street, London EC1V 9EL, UK. [4]Department of Internal Medicine I, University Hospital, Hugstetter Strasse 55, 79106 Freiburg and Institute of Molecular Medicine and Cell Research, Albert-Ludwigs-University, Stefan-Meier-Strasse 17, 79104 Freiburg, Germany. [5]National Center for Tumor Diseases (NCT), Im Neuenheimer Feld 350, 69120 Heidelberg, Germany. [6]Department of Anatomy and Developmental Biology, University College London, Gower Street, London WC1E 6BT, UK. [7]Cincinnati Children's Research Foundation, Molecular and Gene Therapy Program, 3333 Burnet Avenue, Cincinnati, Ohio 45229-3039, USA. [8]Kellogg Eye Center, 1000 Wall Street, Room 541, Ann Arbor, Michigan 48105, USA. [9]Department of Immunology, Great Ormond Street Hospital for Children NHS Trust, London WC1N 3JH, UK. [10]Present address: Nuclear Biology Group, Department of Medical and Molecular Genetics, King's College London School of Medicine, Guy's Tower, Guy's Hospital, London SE1 9RT, UK. [11]These authors contributed equally to this work. Correspondence should be addressed to R.J.Y.-M. (rafael.yanez@genetics.kcl.ac.uk) or R.R.A. (r.ali@ucl.ac.uk).

Received 11 November 2005; accepted 9 January 2006; published online 19 February 2006; doi:10.1038/nm1365

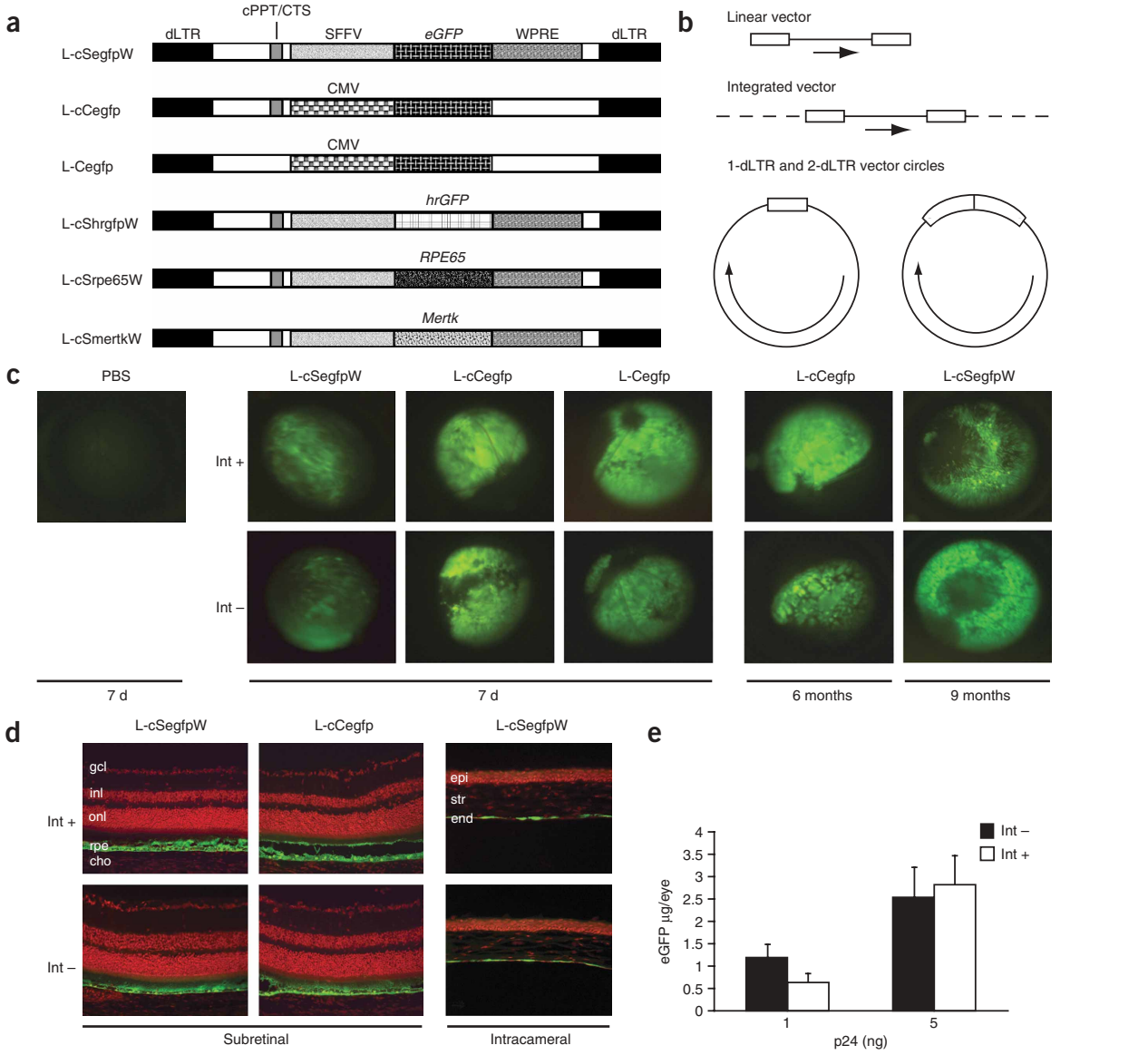

Figure 1 Efficient *in vivo* expression of *eGFP* from integration-deficient vectors in mouse ocular tissues. (**a**) Schematic representation of HIV-1 vectors used in this study. We show double-stranded DNA vector forms after completion of reverse transcription. L, lentiviral vector; c, central polypurine tract–central termination sequence (cPPT/CTS); S, spleen focus-forming virus (SFFV) 3′ LTR promoter; C, cytomegalovirus (CMV) immediate-early promoter; W, woodchuck post-transcriptional regulatory element (WPRE). We have named relevant features on L-cSegfpW and those differing on the other vectors. dLTR is the 5′-deleted LTR present in these self-inactivating vectors. Not drawn to scale. (**b**) Schematic representation of linear, integrated and circular forms of a generic lentiviral vector. Solid lines, vector DNA; dashed lines, genomic DNA; white boxes, dLTRs. Arrows represent the transgene cassettes in the corresponding vector forms. (**c**) *In vivo* eGFP fluorescence at various time points after subretinal injection with the indicated vectors. Int+, integration-proficient; Int–, integration-deficient. (**d**) eGFP fluorescence in cryosections of mouse retina and cornea 6 months after vector administration. We counterstained the sections with propidium iodide (red). Gcl, ganglion cell layer; inl, inner nuclear layer; onl, outer nuclear layer; rpe, retinal pigment epithelium; cho, choroid; epi, corneal epithelium; str, stroma; end, corneal endothelium. (**e**) Dose response of *in vivo* expression of *eGFP* measured by ELISA for eGFP after subretinal vector injection. Error bars, s.e.m.

using integration-proficient lentiviral vectors[19–21]. *In vivo* fluorescence imaging of mouse fundi and postmortem sections showed expression of *eGFP* in the retinal pigment epithelium (RPE) after subretinal injection (**Fig. 1c**,**d**). eGFP fluorescence in the neurosensory retina originated from detached RPE microvilli. Injections in the anterior chamber led to expression predominantly in corneal endothelial cells (**Fig. 1d**) and trabecular meshwork (data not shown). Expression of *eGFP* was highly efficient by 7 d and stable for the duration of the experiments (up to 9 months; **Fig. 1c**). We obtained similar results in rats (**Supplementary Note** and **Supplementary Fig. 2** online). These data show that integration-deficient HIV-1 vectors can mediate long-term, high-level transgene expression *in vivo*. Additional *in vitro* experiments showed that integration-deficient HIV vectors are also proficient at transducing human RPE (**Supplementary Note** and **Supplementary Fig. 3** online).

To compare the transduction efficiency of integration-proficient and integration-deficient vectors, we performed dose-response experiments *in vivo*. We injected mice subretinally with nonsaturating

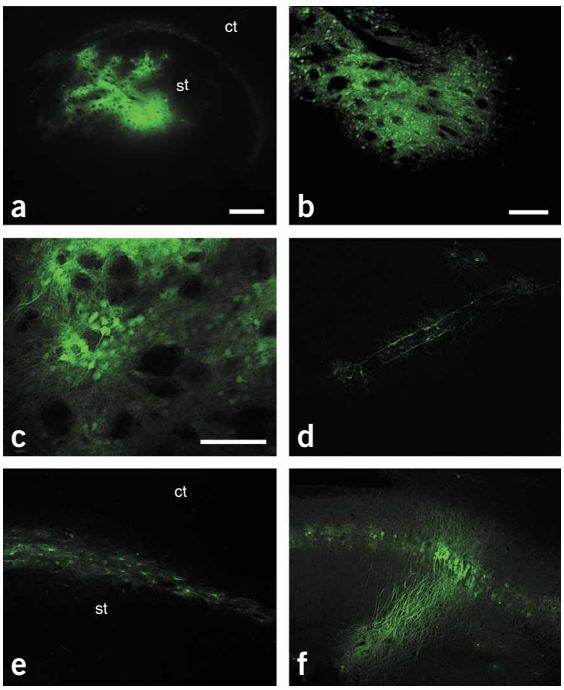

Figure 2 Efficient expression of *eGFP* from integration-deficient vectors in mouse brain. We show eGFP fluorescence in coronal sections of mouse brain, 1 month after injection of integration-deficient L-cCegfp vector. (**a–e**) Corpus striatum, (**f**) hippocampus. (**a**) Low-power micrograph showing eGFP fluorescence after injection into the corpus striatum (st). The cerebral cortex (ct) shows little fluorescence, indicating that there was no retrograde transduction of corticostriate projection neurons. Scale bar, 40 μm. (**b**) Higher-power image showing densely packed fluorescent cell bodies in the striatum. (**c**) Morphological identification of most of the cell bodies expressing *eGFP* in the striatum as neurons. Scale bar, 10 μm. (**d**) Blood vessel in the striatum, approximately 1 mm from the injection site. The vector spread along the outside of blood vessels, transducing perivascular astrocytes and some endothelial cells. (**e**) The vector also spread in the plane of white matter as shown by the transduced glia in the subcortical white matter separating cerebral cortex and striatum. (**f**) Transduced neurons near an injection site in the hippocampus. Scale bars in **b** and **d–f**, 20 μm.

amounts of integration-proficient or integration-deficient vectors encoding *eGFP* and measured eGFP levels by ELISA. The differences between integration-proficient and integration-deficient vectors injected at equivalent doses were not statistically significant. This result was consistent in two separate experiments (combined in **Fig. 1e**). We conclude that efficient *eGFP* expression can be achieved *in vivo* with integration-deficient vectors.

To test the ability of integration-deficient vectors to transduce other tissues, we performed stereotactic injections of paired *eGFP*-expressing vectors into corpus striatum and hippocampus in mice. We analyzed brains 7 and 30 d after injection. eGFP fluorescence was more widespread at the latter time point. Transduction efficiency and spatial transduction patterns were similar regardless of integration proficiency (data not shown). Many cells of the corpus striatum showed bright eGFP fluorescence, with neurons more commonly transduced than glia and no signs of retrograde neuronal transduction (**Fig. 2a–e**). Most of the transduced striatal cells were medium spiny-projection neurons and large aspiny interneurons (**Fig. 2b**,**c**). The vector spread along the outside of blood vessels, and in the white matter, transduction of endothelial and glial cells was more efficient (**Fig. 2d**,**e**). In the hippocampus, we detected fluorescent neurons in the hilus of the dentate gyrus and the CA3 region (**Fig. 2f**), and strongly fluorescent glia in the fimbria (data not shown).

We examined the ability of integration-deficient lentiviral vectors to correct genetic diseases using rodent models of retinal dystrophies. *Rpe65*$^{rd12/rd12}$ mutant mice have a phenotype similar to that of individuals with Leber congenital amaurosis, a severe form of early-onset autosomal recessive retinitis pigmentosa that results from mutations in *RPE65* (ref. 22). Rescue of mouse *Rpe65* deficiency has been previously reported[23]. Subretinal delivery of an integration-deficient vector carrying a functional human *RPE65* transgene led to expression of *RPE65* in transduced RPE (**Fig. 3a**). Functional rescue was assessed by electroretinography (ERG), which measures the electrical response of the entire retina to a light stimulus[24]. We observed substantial improvements in ERG waveform (**Fig. 3b**) and significant improvements in b-wave amplitude ($P = 0.001$ at a flash intensity of 100 mcds/m^2, $P = 0.007$ at 1,000 mcds/m^2; **Fig. 3c**) 3 weeks after injection of integration-deficient *RPE65* vector. The b-wave response at 100 mcds/m^2 was almost sixfold greater in vector-treated eyes than in untreated contralateral eyes (**Fig. 3c**). We observed similar improvements in electrical response in eyes treated with integrase-deficient or integrase-proficient *RPE65* vector (**Fig. 3b**,**c**). These improvements were stable for at least 8 weeks after injection (latest time point studied; **Fig. 3d**,**e**). The mean b-wave amplitude measured in integration-deficient *RPE65* vector-treated mice was approximately 50% of wild-type values (data not shown). We observed no significant improvement after injection of control *hrGFP* vector (**Fig. 3b**,**c**). Integration-deficient vectors encoding *Mertk* were similarly efficient at rescuing the Royal College of Surgeons rat model of retinitis pigmentosa (**Supplementary Note** and **Supplementary Fig. 4** online). These results show that integration-deficient vectors can produce substantial functional rescue of clinically relevant disease models.

We sought to provide evidence that *in vivo* transgene expression in eyes injected subretinally with integration-deficient vectors originated from unintegrated vector templates. Using specific quantitative real-time PCR (qPCR), we measured molecules containing a junction of the two 5′-deleted LTRs (2-dLTR) present in these self-inactivating vectors, and total vector molecules. We found that the ratio of 2-dLTR/total vector DNA in mouse and rat eyecup samples combined was on average eightfold higher with integration-deficient vectors than with their integrating counterparts, and that this was stable over time (**Fig. 4a**). These data indicate that 2-dLTR vector forms persist in eyes injected with integration-deficient vectors, but do not exclude the possibility that they could have integrated with that configuration. Given that genomic integration of circular vector forms could occur through DNA breaks located anywhere in the vector circle, we used linear amplification-mediated (LAM)-PCR[25] to scan three regions of the vector DNA (approximately 30–50% of the vector genome depending on vector size) for vector-host DNA junctions (**Fig. 4b**). We easily detected dLTR-host DNA junctions in eyes injected with integration-proficient vectors (**Supplementary Table 2** online). In contrast, an extensive search for integration junctions in eyes injected with integration-deficient vectors showed a single detectable integration event (out of 815 LAM-PCR amplicons sequenced; **Supplementary Table 2** online). The sequence at this unique integration junction was that expected from a dLTR-mediated integration event. Therefore, the extensive ocular expression of reporter and therapeutic genes that we have shown with integration-deficient

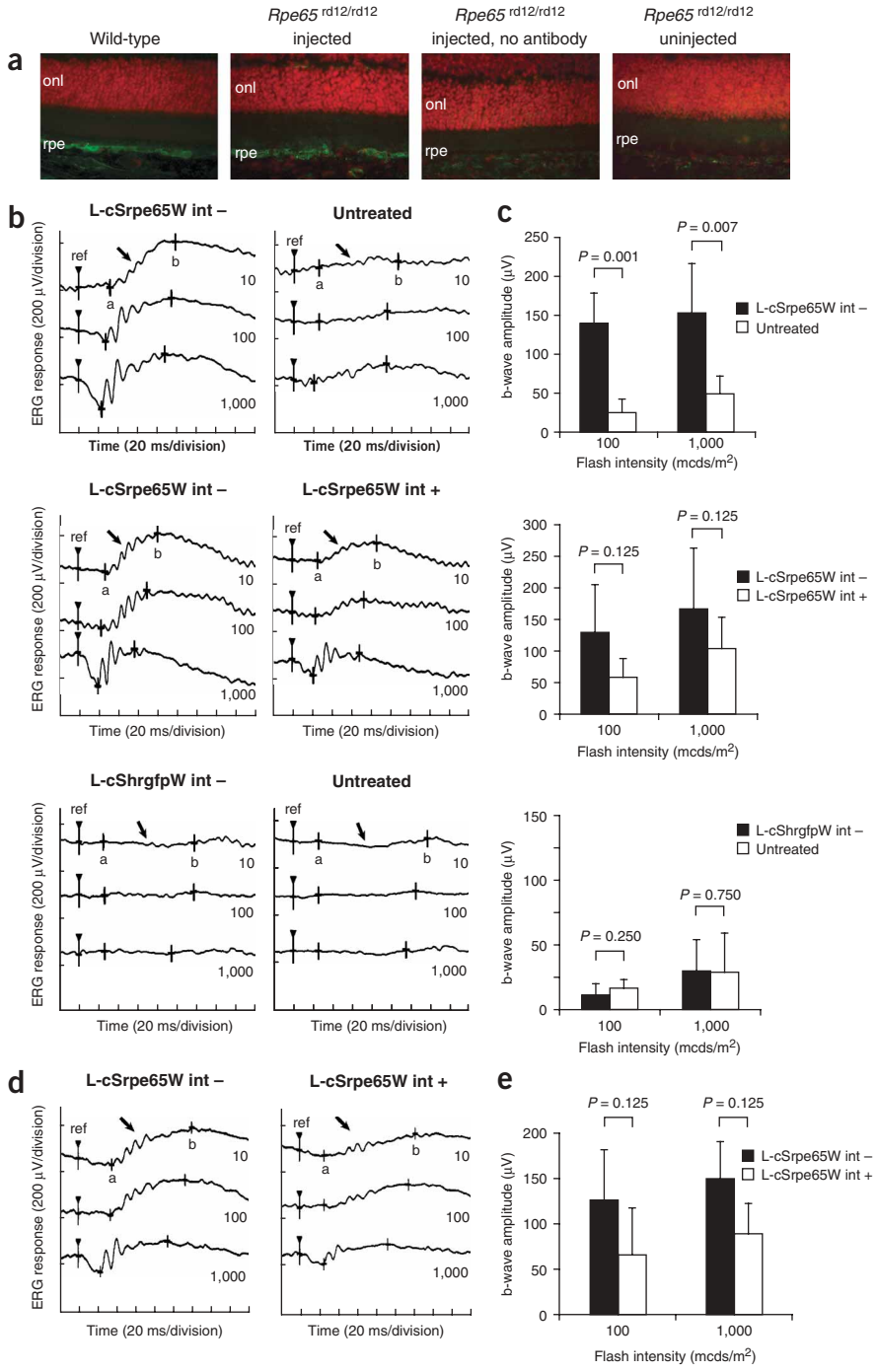

Figure 3 Rescue of ocular function in *Rpe65*$^{rd12/rd12}$ mice. (**a**) Subretinal delivery of L-cSrpe65W results in efficient *RPE65* expression in mouse RPE. We immunostained retinal cryosections for RPE65 (green) and counterstained with propidium iodide (red). We show RPE65 immunohistochemical labeling in the RPE layer of wild-type mice and in *Rpe65*$^{rd12/rd12}$ mice 3 weeks after subretinal injection of integrase-deficient L-cSrpe65W. RPE65 is not detected in sections from L-cSrpe65W–injected *Rpe65*$^{rd12/rd12}$ mice incubated without primary antibody nor in uninjected *Rpe65*$^{rd12/rd12}$ mice. Some background fluorescence from the secondary antibody is visible in the choroid and sclera in all sections. onl, outer nuclear layer; rpe, retinal pigment epithelium. (**b**) Sample scotopic ERG traces at flash intensities of 10, 100 and 1,000 mcds/m^2 from *Rpe65*$^{rd12/rd12}$ eyes injected with integration-deficient L-cSrpe65W and untreated contralateral eyes, integration-deficient and -proficient L-cSrpe65W, and integration-deficient L-cShrgfpW and untreated contralateral eyes, 3 weeks after subretinal vector administration. Ref, reference value; a, a-wave trough; b, b-wave peak. Arrow indicates b-wave. (**c**) Mean ERG b-wave amplitudes of the same paired groups. Error bars, s.d. int –, integration deficient; int +, integration proficient. (**d**,**e**) We observed similar improvements in ERG waveform and b-wave amplitude in *Rpe65*$^{rd12/rd12}$ mice injected with integration-deficient or -proficient L-cSrpe65W for at least 8 weeks after injection.

vector components for successful *in vivo* transduction. Compared to other nonintegrating vectors, perhaps the main potential advantages of integration-deficient lentiviral vectors are their greater transgene capacity (with respect to recombinant adeno-associated virus vectors) and their low immunogenicity.

Combining the high efficiency of gene transfer mediated by lentiviruses with a stable nonintegrating vector system is highly attractive for safe clinical application. For long-term gene expression, quiescence of the target-cell population is a requisite, as episomes do not otherwise persist in the absence of effective origins of replication. But many tissues including muscle, liver, brain and retina are essentially postmitotic, particularly in adults, and are targets for the development of diverse gene therapy strategies. Even in tissues where transformation of target cells is unlikely, the risks associated with inadvertent transduction of bystander cells or other cells (including germ cells) as a result of vector spread during *in vivo* administration are substantially reduced.

vectors is most likely to derive from transcriptionally proficient, unintegrated vector episomes.

Insertional mutagenesis can be avoided by the use of gene therapy vectors that do not integrate. Lentiviral vectors have recently come to prominence because of their efficiency of cell transduction, including transduction of postmitotic cells, and paucity of immune recognition[12,26]. Here we show for the first time that integration-deficient HIV-1–based vectors mediate sustained gene expression *in vivo*, and have the capacity to rescue representative models of clinical disease. Although these findings conflict with previous studies[14–16], we have been unable to determine dependence on species or

The demonstration of efficient *in vivo* transduction with integrase-deficient HIV-1 vectors points to their potential application in human gene therapy, for which an effective vector with highly reduced risk of genomic integration has clear biosafety advantages. We suggest that integration-defective lentiviruses should be evaluated preferentially over their integrating counterparts for gene therapy of diseases of postmitotic tissues.

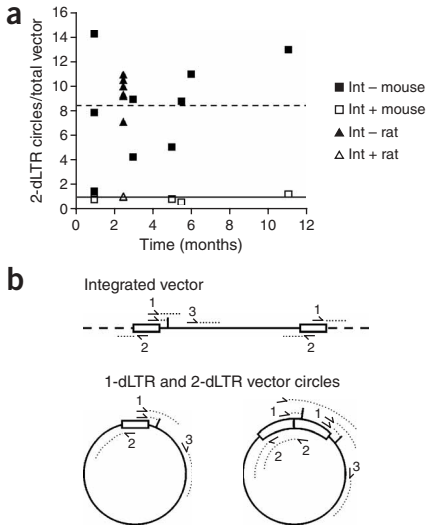

Figure 4 Analyses of HIV vector integration *in vivo*. (**a**) qPCR quantification of 2-dLTR junction-containing molecules in transduced eyecups. We injected mouse eyes with L-cSegfpW or L-cCegfp, and rat eyes with L-cSmertkW. We show a normalized ratio 2-dLTR molecules/total vector. We arbitrarily set to 1 the average ratio for integration-proficient (Int +) vectors (solid line). The average ratio for integration-deficient (Int –) vectors is indicated by a dashed line. (**b**) Strategy for detection of vector-host DNA junctions by LAM-PCR. We designed three different LAM-PCR reactions to scan vector regions downstream of the 5′-dLTR (1), upstream of the 3′-dLTR (2) and downstream of residual *env* sequences (a region including cPPT/CTS and internal promoter, 3) for integration junctions. Reactions 1 and 2 would also detect normal dLTR-host DNA junctions. The vector region scanned with each LAM-PCR reaction spans from the corresponding forward oligonucleotide of the second exponential PCR to the first downstream restriction site for the enzyme used. We estimate the length of each scanned region to be between 600 and 1,000 bp if there is no intervening restriction site. Schematic representations of integrated (through normal LTR-mediated integration) and circular forms of a generic lentiviral vector are shown. Solid lines, vector DNA; dashed lines, genomic DNA; white boxes, dLTRs. Also indicated is the forward oligonucleotide of the second exponential PCR for each of the LAM-PCR assays (numbered arrows), the region potentially scanned with each assay (dotted lines) and relevant *Tsp*509I sites (solid lines interrupting some reactions with primer set 1).

METHODS

For details of Methods, please see **Supplementary Methods** online.

Plasmids. HIV-1 plasmids pD64VintCMVDR9 (mutant integrase), pCMVdR8.74, pMDLg/pRRE, pRSV.REV and pMD2VSV.G have been previously described[12,18]. We made integrase-deficient second- and third-generation plasmids pCMVdR8.74intD64V and pMDLg/pRREintD64V by cloning an *Afl*II/*Bcl*I fragment spanning the integrase mutation from pD64VintCMVDR9 into *Afl*II/*Bcl*I-digested pCMVdR8.74 and pMDLg/pRRE, respectively. Lentiviral transfer plasmids pHR'SIN-cPPT-SEW, pHR'SIN-CE, pHR'SIN-cPPT-CE and LNT.SFFV.Mertk have been previously described[27,28] and we used them to make the vectors L-cSegfpW, L-Cegfp, L-cCegfp and L-cSmertkW, respectively. We used transfer plasmids pHR'SIN-cPPT-ShrgfpW (carrying the *hrGFP* gene) and pHR'SIN-cPPT-Srpe65W (containing a human *RPE65* transgene) to prepare the vectors L-cShrgfpW and L-cSrpe65W, respectively.

Cells. We cultured HeLa and 293T cells in DMEM with standard supplements. Details on culture and transduction of human RPE cells are in **Supplementary Methods** online.

Vector production, purification and titration. We produced HIV vectors by transient transfection and pseudotyped them with the vesicular stomatitis virus glycoprotein G envelope as described[27]. We performed p24 titrations using Beckman Coulter kits PN6604535 and PN626391, following the manufacturer's instructions. For eGFP and qPCR titrations, we transduced HeLa cells with serial dilutions of vector stock in the presence of 8 μg/ml polybrene. We scored $eGFP^+$ cells using FACS analysis. We carried out qPCR titrations of total vector DNA according to a published protocol for late reverse transcriptase amplicon quantification[29] but, to compare integration-proficient and integration-deficient vectors, we harvested cells 24 h after transduction. We purified DNA using the DNAeasy kit (Qiagen). We normalized qPCR values by quantifying copies of the gene encoding actin in the DNA extracts and correcting for HeLa cell aneuploidy.

Molecular analyses of vector forms in injected eyes. We performed qPCR and LAM-PCR analyses on eyecup DNA prepared using the DNAeasy kit (Qiagen). We carried out a 2-dLTR junction qPCR assay for self-inactivating HIV vectors using the following oligonucleotide sequences: 2-dLTR forward, 5′-AACTAGA GATCCCTCAGACCCTTTT-3′; 2-dLTR reverse, 5′-CTTGTCTTCGTTGGG AGTGAATT-3′; and a Taqman MGB probe, 5′-FAM-CTAGAGATTTTCCA CACTGAC-3′. We performed LAM-PCR as previously described[25] with some modifications (**Supplementary Methods** online).

Intraocular injections. We treated all animals using procedures approved by the UK Home Office and the Institute of Ophthalmology Research Ethics Committee, and in compliance with the Association for Research in Vision and Ophthalmology Statement for the Use of Animals in Ophthalmic and Vision Research. We performed subretinal injections as previously described[19].

Ocular eGFP imaging in mice. Adult female C57Bl/6J mice received *eGFP* vectors (**Supplementary Table 3** online). We visualized *in vivo* expression of *eGFP* using a modified human ophthalmic slit lamp. We imaged mice 1 week (all *eGFP* constructs), between 1 and 6 months (L-cSegfpW and L-cCegfp constructs) and at 9 months after injection (L-cSegfpW). We also analyzed expression of *eGFP* using fluorescence microscopy on cryosections obtained between 3 d and 6 months after injection.

eGFP ELISA. We injected mouse eyes ($n = 6$–8 per group in the first experiment, $n = 8$ per group in the second experiment) subretinally with 1 or 5 ng p24 of integration-proficient or integration-deficient vectors encoding *eGFP* and harvested eyes 11 d later. We prepared whole-eye extracts and used clarified supernatant for ELISA following standard procedures. We captured eGFP using a monoclonal antibody (ab1218-100, 1:10,000 dilution; Abcam) and used recombinant eGFP (Clontech) as a standard for absolute quantification of eGFP.

Brain injections and histological analysis. We injected adult female C57Bl/6J mice with 0.8 μl (6.50×10^8 eGFP transducing units/ml) of integration-proficient or integration-deficient L-cCegfp vectors over 25 min into the striatum ($n = 5$) or the hippocampal formation ($n = 2$). We retrieved brains at 7 and 30 d after injection, mounted 40 μm-thick coronal cryosections in DABCO and examined them with a fluorescence microscope. We followed procedures approved by the University College London Ethical Committee and the UK Home Office.

Rescue of *Rpe65* deficiency in mice. Five-week-old $Rpe65^{rd12/rd12}$ mice received unilateral subretinal injections of either integration-deficient L-cSrpe65W (46.5 ng/μl p24; $n = 6$) or L-cShrgfpW (45.0 ng/μl p24; $n = 3$); we left contralateral eyes untreated. Additional mice ($n = 4$) received unilateral injections of integration-deficient L-cSrpe65W; contralateral eyes received integration-proficient L-cSrpe65W (70 ng/μl p24). We performed ERG analysis 3 or 8 weeks later as previously described[30]. This study design controls for the interanimal and test-retest variability inherent in rodent ERGs. We killed some animals 3 weeks after injection for RPE65 immunohistochemistry (**Supplementary Methods** online).

Statistical analyses. We analyzed ELISA measurements of eGFP levels for statistical significance ($P < 0.05$) using the one-way nonparametric Kruskal-Wallis test with Dunn correction. For ERG measurements, we compared b-wave amplitudes from contralateral eyes. As ERG amplitude data do not follow a normal distribution, we used a nonparametric test for paired samples

(Wilcoxon matched-pairs test) to evaluate significance ($P < 0.05$). We performed statistical analyses with GraphPad Prism software.

Note: Supplementary information is available on the Nature Medicine website.

ACKNOWLEDGMENTS

The authors thank L. Naldini for lentiviral plasmids, M. Balda for ARPE-19 cells, S. Wilkie for human *RPE65* cDNA, D. Thompson for RPE65-specific antibody and D. King for human actin plasmid. This work was supported by the Wellcome Trust (A.J.T. and R.J.Y.-M.), the Sir Jules Thorn Charitable Trust (A.J.T. and R.R.A.), the Special Trustees of Moorfields Eye Hospital (R.R.A.) and the European Union Integrated Project CONSERT (Concerted Safety and Efficiency of Retroviral Transgenesis in Gene Therapy of Inherited Diseases) 005242 (C.v.K., A.J.T. and S.J.H.).

COMPETING INTERESTS STATEMENT

The authors declare competing financial interests (see the *Nature Medicine* website for details).

Published online at http://www.nature.com/naturemedicine/
Reprints and permissions information is available online at http://npg.nature.com/reprintsandpermissions/

1. Baum, C. *et al.* Side effects of retroviral gene transfer into hematopoietic stem cells. *Blood* **101**, 2099–2114 (2003).
2. Li, Z. *et al.* Murine leukemia induced by retroviral gene marking. *Science* **296**, 497 (2002).
3. Hacein-Bey-Abina, S. *et al. LMO2*-associated clonal T cell proliferation in two patients after gene therapy for SCID-X1. *Science* **302**, 415–419 (2003).
4. Saenz, D.T. *et al.* Unintegrated lentivirus DNA persistence and accessibility to expression in nondividing cells: analysis with class I integrase mutants. *J. Virol.* **78**, 2906–2920 (2004).
5. Vargas, J., Jr., Gusella, G.L., Najfeld, V., Klotman, M.E. & Cara, A. Novel integrase-defective lentiviral episomal vectors for gene transfer. *Hum. Gene Ther.* **15**, 361–372 (2004).
6. Lu, R. *et al.* Simian virus 40-based replication of catalytically inactive human immunodeficiency virus type 1 integrase mutants in nonpermissive T cells and monocyte-derived macrophages. *J. Virol.* **78**, 658–668 (2004).
7. Engelman, A. *In vivo* analysis of retroviral integrase structure and function. *Adv. Virus Res.* **52**, 411–426 (1999).
8. Shank, P.R. *et al.* Mapping unintegrated avian sarcoma virus DNA: termini of linear DNA bear 300 nucleotides present once or twice in two species of circular DNA. *Cell* **15**, 1383–1395 (1978).
9. Hsu, T.W., Sabran, J.L., Mark, G.E., Guntaka, R.V. & Taylor, J.M. Analysis of unintegrated avian RNA tumor virus double-stranded DNA intermediates. *J. Virol.* **28**, 810–818 (1978).
10. Pierson, T.C. *et al.* Intrinsic stability of episomal circles formed during human immunodeficiency virus type 1 replication. *J. Virol.* **76**, 4138–4144 (2002).
11. Butler, S.L., Johnson, E.P. & Bushman, F.D. Human immunodeficiency virus cDNA metabolism: notable stability of two-long terminal repeat circles. *J. Virol.* **76**, 3739–3747 (2002).
12. Naldini, L. *et al. In vivo* gene delivery and stable transduction of nondividing cells by a lentiviral vector. *Science* **272**, 263–267 (1996).
13. Case, S.S. *et al.* Stable transduction of quiescent CD34(+)CD38(-) human hematopoietic cells by HIV-1-based lentiviral vectors. *Proc. Natl. Acad. Sci. USA* **96**, 2988–2993 (1999).
14. Naldini, L., Blomer, U., Gage, F.H., Trono, D. & Verma, I.M. Efficient transfer, integration, and sustained long-term expression of the transgene in adult rat brains injected with a lentiviral vector. *Proc. Natl. Acad. Sci. USA* **93**, 11382–11388 (1996).
15. Loewen, N. *et al.* Comparison of wild-type and class I integrase mutant-FIV vectors in retina demonstrates sustained expression of integrated transgenes in retinal pigment epithelium. *J. Gene Med.* **5**, 1009–1017 (2003).
16. Park, F., Ohashi, K. & Kay, M.A. Therapeutic levels of human factor VIII and IX using HIV-1-based lentiviral vectors in mouse liver. *Blood* **96**, 1173–1176 (2000).
17. Leavitt, A.D., Robles, G., Alesandro, N. & Varmus, H.E. Human immunodeficiency virus type 1 integrase mutants retain *in vitro* integrase activity yet fail to integrate viral DNA efficiently during infection. *J. Virol.* **70**, 721–728 (1996).
18. Dull, T. *et al.* A third-generation lentivirus vector with a conditional packaging system. *J. Virol.* **72**, 8463–8471 (1998).
19. Bainbridge, J.W. *et al. In vivo* gene transfer to the mouse eye using an HIV-based lentiviral vector; efficient long-term transduction of corneal endothelium and retinal pigment epithelium. *Gene Ther.* **8**, 1665–1668 (2001).
20. Bemelmans, A.P. *et al.* Retinal cell type expression specificity of HIV-1-derived gene transfer vectors upon subretinal injection in the adult rat: influence of pseudotyping and promoter. *J. Gene Med.* **7**, 1367–1374 (2005).
21. Gruter, O. *et al.* Lentiviral vector-mediated gene transfer in adult mouse photoreceptors is impaired by the presence of a physical barrier. *Gene Ther.* **12**, 942–947 (2005).
22. Pang, J.J. *et al.* Retinal degeneration 12 (rd12): a new, spontaneously arising mouse model for human Leber congenital amaurosis (LCA). *Mol. Vis.* **11**, 152–162 (2005).
23. Dejneka, N.S. *et al. In utero* gene therapy rescues vision in a murine model of congenital blindness. *Mol. Ther.* **9**, 182–188 (2004).
24. Smith, A.J. *et al.* AAV-Mediated gene transfer slows photoreceptor loss in the RCS rat model of retinitis pigmentosa. *Mol. Ther.* **8**, 188–195 (2003).
25. Schmidt, M. *et al.* Polyclonal long-term repopulating stem cell clones in a primate model. *Blood* **100**, 2737–2743 (2002).
26. Abordo-Adesida, E. *et al.* Stability of lentiviral vector-mediated transgene expression in the brain in the presence of systemic antivector immune responses. *Hum. Gene Ther.* **16**, 741–751 (2005).
27. Demaison, C. *et al.* High-level transduction and gene expression in hematopoietic repopulating cells using a human imunodeficiency virus type 1-based lentiviral vector containing an internal spleen focus forming virus promoter. *Hum. Gene Ther.* **13**, 803–813 (2002).
28. Tschernutter, M. *et al.* Long-term preservation of retinal function in the RCS rat model of retinitis pigmentosa following lentivirus-mediated gene therapy. *Gene Ther.* **12**, 694–701 (2005).
29. Butler, S.L., Hansen, M.S. & Bushman, F.D. A quantitative assay for HIV DNA integration *in vivo*. *Nat. Med.* **7**, 631–634 (2001).
30. Ali, R.R. *et al.* Restoration of photoreceptor ultrastructure and function in retinal degeneration slow mice by gene therapy. *Nat. Genet.* **25**, 306–310 (2000).